Desalination and Water Treatment
www.deswater.com
doi: 10.1080/19443994.2015.1119753

57 (2016) 21314–21327
September

Taylor & Francis
Taylor & Francis Group

Feasibility study of flowback/produced water treatment using direct-contact membrane distillation

Guiying Rao[a], Ying Li[b,c,*]

[a]*Mechanical Engineering Department, University of Wisconsin-Milwaukee, 3200 N Cramer St, Milwaukee, WI 53211, USA, Tel. +1 775 338 0433; email: raog@uwm.edu*
[b]*Department of Mechanical Engineering, Texas A&M University, 3123 TAMU, College Station, TX 77843, USA, Tel. +1 979 862 4465; email: yingli@tamu.edu*
[c]*Water Technology Accelerator (WaTA), University of Wisconsin-Milwaukee, 247 W Freshwater Way, Milwaukee, WI 53204, USA*

Received 28 May 2015; Accepted 4 November 2015

ABSTRACT

The feasibility of applying direct-contact membrane distillation (DCMD) for flowback/produced water treatment was comprehensively investigated under different hydrodynamic and thermal conditions with various feedwater compositions. Results from a bench-scale study suggest that DCMD has a great potential to treat synthetic flowback/produced water. Membrane water flux increased with increasing feedwater temperature. At a feedwater temperature of 80°C, TDS of 133 g/L and liquid stream flow rates of 0.8 L/min, DCMD showed a water flux as high as 43 L/m^2 h, which is comparable to water fluxes of reverse osmosis (RO) for seawater desalination. In addition, DCMD is capable of treating flowback/produced water with TDS up to 280 g/L, leading to 46–88% reduction of wastewater volume. Oil/grease, suspended solids, and volatile organics in the synthetic flowback/produced water showed minimal effects on DCMD performance; thus, no pretreatment process is necessary in DCMD. The high-quality distillate of DCMD may be used for beneficial reuse or future hydraulic fracking jobs. However, it is not recommended to treat low-TDS flowback/produced water that can be processed by RO. Rather, DCMD has more technical advantages for treating medium- and high-TDS flowback/produced water.

Keywords: Direct-contact membrane distillation; Flowback/produced water; Total dissolved solids; Water reuse; Feasibility analysis

1. Introduction

Flowback and produced water are two important water streams associated with oil and gas production. Flowback water refers to the wastewater flowing back to wellbores after the hydraulic fracturing process [1]. During hydraulic fracturing, large quantities of fracking fluids—a mixture of sand, chemical additives, and fresh water withdrawn from surface and groundwater resources—are injected into wellbores under high pressure [1], and a fraction of the fracking fluids may flow back to the wellbore within a few weeks after hydraulic fracturing [2]. Naturally occurring water found in rock formations may also flow into the wellbore throughout the oil and gas production

*Corresponding author.

process and this water is referred to as produced water [3]. It was estimated that 10.5 billion gallons of flowback/produced water were generated globally each day [4]. Public concerns of flowback/produced water are increasing due to its environmental impacts, such as the depletion of freshwater supplies, groundwater contamination, and air pollution. Flowback/produced water typically contains organics, suspended solids, and dissolved inorganics. Among the inorganics, sodium and chloride have the highest concentrations [3,5]; calcium, barium, strontium, bicarbonate, sulfate, bromide, and radionuclides are also commonly present [5,6]. Oil and grease may float on water surface or disperse into the water and form oil-in-water emulsions.

Due to the demand of large quantities of fracking fluids and the water scarcity, reuse of flowback/produced water is becoming dominant [7]. A portion of flowback/produced water may be reused directly as long as it meets the water quality of the end use. While reusing flowback/produced water for beneficial purposes such as for agricultural activities (the largest use of fresh water in USA [8]) requires TDS-reduction treatment processes because of the much lower recommended TDS for beneficial use (1,000–2,000 mg/L [9]) than the TDS of typical flowback/produced water. The flowback/produced water can also be reused for future hydraulic fracturing jobs if it contains low concentrations of TDS and total suspended solids (TSS) with low scaling tendency [10]. The water not suitable for reuse is currently disposed of by underground injection wells, which costs $1.5–2.0/bbl for disposal and up to $4.0/bbl if including transportation [11]. Therefore, it is desirable to decrease the concentrations of TDS, TSS, and scaling ions to facilitate the reuse of flowback/produced water. Removing suspended solids and scaling ions can be achieved through simple filtration and precipitation processes [12], while removal of TDS is relatively difficult and the coexistence of various contaminants necessitates multiple treatment technologies consecutively [10]. Jiang et al. [13] developed a two-stage ceramic microfiltration system coupled with a mixed bed ion-exchange system and successfully reduced the TDS of the flowback/produced water from 48 g/L to less than 500 mg/L. Forward osmosis (FO) was also applied in the laboratory and onsite for flowback/produced water treatment [1,14–16] but membrane fouling was reported even when the feedwater was pretreated by ultrafiltration [14]. Also, an additional system (e.g. vacuum membrane filtration [17]) for regeneration of draw solution of FO is required [18], resulting in a more complicated process and increased capital cost.

Membrane distillation (MD) is also a potential technology for flowback/produced water treatment. MD is a thermally driven process in which phase change of water from liquid to vapor occurs on the membrane surface to separate water from contaminants and produce low-TDS distillate. The driving force of MD is the vapor pressure gradient resulting from the temperature gradient across the membrane. MD can utilize solar energy, geothermal energy, and industrial waste heat to heat up the feed solution thus reduce energy cost [19–21]. MD has been successfully used to treat high-TDS feed solutions, such as industrial wastewater [22,23], water from salty lakes [24], and reverse osmosis (RO) brines [25,26], and achieved almost 100% salt and nonvolatile organic rejection despite the fouling and scaling potentials of the feed solutions [27]. A pilot plant combining ultrafiltration/RO and air-gap MD has been applied to treat low TDS (14.1 g/L) flowback/produced water [28]. The capability of air-gap MD to treat high-TDS wastewater has yet to be demonstrated. Although the treatment of high-TDS (187 g/L) flowback/produced water was reported in another study using air-gap MD, a water flux of only 8 L/m^2 h was reported [29], which is relatively low in comparison with direct-contact membrane distillation (DCMD) [30,31]. In DCMD, two water streams at different bulk temperatures are circulated on either side of a hydrophobic microporous membrane. The temperature of the feed solution ranges from 30 to 90°C [27,32] and that of the distillate ranges from 25 to 30°C [33,34]. To date, few studies have been performed using DCMD to treat flowback/produced water. Singh and Sirkar [35] investigated the effect of temperature on water flux and organic removal using DCMD for the treatment of simulated produced water, which had a relatively high temperature (95–125°C), very low TDS (only 3,000 mg/L NaCl), and 10–45 mg/L organics without the presence of oil/grease, scaling ions, and suspended solids that are commonly found in real produced water. Macedonio et al. [36] investigated the effects of temperature and flow rate on DCMD performance for produced water treatment. The feedwater had a fixed composition with a total organic carbon of 18.1 mg/L (with only 1,2-diethoxy ethane inside), TDS of 247.9 g/L, and suspended solids of 300 mg/L. In addition, the produced water was pretreated by microfiltration and activated carbon filtration; thus, the effect of organics on DCMD performance was unknown. The same problem also occurred in the study with oily wastewater pretreated by the FO process before DCMD [37]. The above literature review indicates the lack of a systematical investigation of the effects of experimental conditions and compositions of flowback/produced

water (e.g. TDS, oil and grease, suspended solids, volatile organics) on DCMD performance. Therefore, the overall objective of this study was to conduct a comprehensive investigation on the technical feasibilities of using DCMD system for flowback/produced water treatment. To achieve this, synthetic flowback/produced water samples were prepared and the effects of feed bulk temperature, flow rate, feedwater TDS, oil/grease, suspended solids, and volatile organic compounds (VOCs) on DCMD performance were studied. Findings from this study are significant to the research community in searching an effective disposal or reuse method for flowback/produced water.

2. Materials and methods

2.1. Chemicals and membranes

Petroleum (18% aromatics basis, Sigma-Aldrich) was used to represent the oil/grease in the flowback/produced water. Sodium chloride (NaCl; 99.9%, Fishier Scientific) and calcium chloride dehydrate ($CaCl_2{\cdot}2H_2O$; >99%, Alfa Aesar) were used as the precursors of dissolved solids. Methanol (>99.8%, Fishier Scientific) was used to represent the VOCs. To mimic the suspended solids, commercial titanium oxide nanopowders (TiO_2 P25, Evonik Degussa), synthetic calcium carbonate ($CaCO_3$), and synthetic barium sulfate ($BaSO_4$) particles were suspended in the feed solution. $CaCO_3$ was prepared by mixing sodium carbonate (Na_2CO_3; >99.5%, Sigma-Aldrich) with the feed solution containing calcium ions. $BaSO_4$ was prepared by mixing barium nitrate (ACS grade, Fishier Scientific) with sodium sulfate (≥99%, Sigma-Aldrich). The synthetic flowback/produced water was prepared by blending the aforementioned chemicals in deionized (DI) water using a Waring™ laboratory blenders (Waring Products Division, USA) for 10 min to form stable oil-in-water emulsions. Two commercially available flat-sheet MD membranes were tested, and the membrane properties are given in Table 1.

Table 1
Properties of commercially available membranes used in this study

Trade name	QM038	GVHP
Manufacturer	Sterlitech, USA	EMD, Millipore Corporation, USA
Material	PTFE[a]	PVDF[a]
Structure	Single-layer	Single-layer
Pore size (μm)	0.20	0.22
Thickness	25–50	125
Porosity (%)	64–82[b]	75
Tortuosity	1.70–2.89[b]	2.08[b]

[a]PTFE—polytetrafluoroethylene; PVDF—polyvinylidene fluoride.
[b]Characterized using the method reported in [38]; other properties were given by the manufacturers.

2.2. Characterization of particle size distribution

Size distributions of oil/grease and suspended solids (TiO_2, $BaSO_4$, and $CaCO_3$) in the synthetic flowback/produced water were characterized by a Nano Series Zetasizer (ZEN3600, Malvern Instruments, UK).

2.3. Experimental setup and procedures

The bench-scale DCMD configuration is given in Fig. 1. The membrane module (CF042, Sterlitech, USA) utilized a flat-sheet membrane with 42 cm^2 surface area. The feed reservoir contained 0.8 L synthetic flowback/produced water with the water level/properties kept the same during each test by adding DI water into the feed reservoir every 10 min. The feedwater was under stirring at 350 rpm during the test to ensure homogeneity of the solution. The distillate reservoir contained 4 L DI water. Both reservoirs were covered by alumina foils to minimize evaporation. Temperature of the feed stream was controlled by a rope heater (FGR-100, Omega Engineering, INC., USA) coupled with a temperature controller (CG-3207, Chemglass, USA). Temperature of the distillate stream was controlled by a recirculating chiller (NESLAB ThermoFlex 1400, Thermo Fisher Scientific, USA). Downstream the membrane module on both feed and distillate sides, a needle valve was used to maintain the same hydraulic pressure (10 ± 2 kPa) in the module on both sides of the membrane (except the tests with varying flow rates). A portable conductivity meter (Traceable™, VWR International, USA) was used to measure the feed and distillate conductivities. Two spacers (Sterlitech, USA) were used, one on the feed side and one on the distillate side of the membrane, to generate turbulence and reduce polarization effects. The feed and distillate streams were circulated counter-currently on their respective sides of the membrane. As water evaporated through the membrane, the excess water from the distillate reservoir overflowed into a beaker on an analytical balance and the overflow rate was used to calculate water flux.

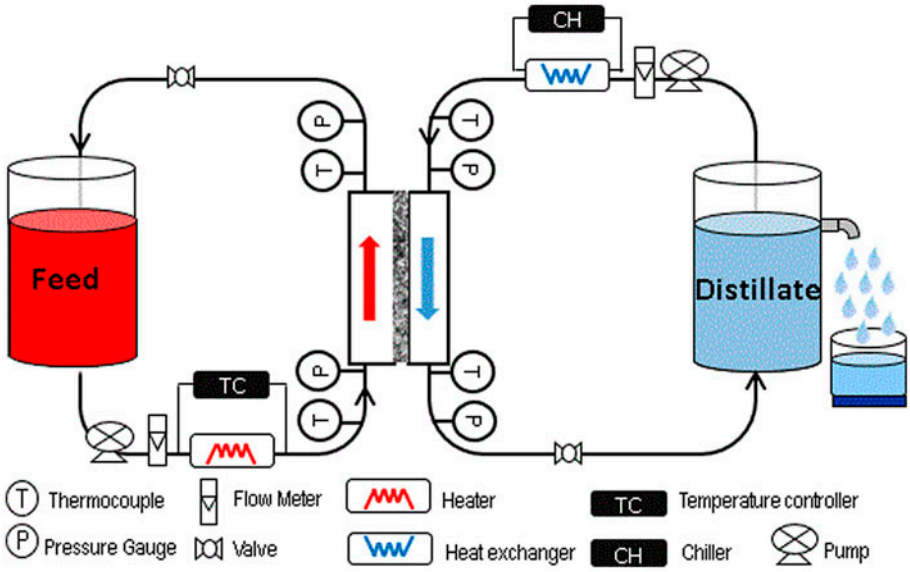

Fig. 1. Schematic diagram of the bench-scale DCMD system.

2.3.1. Effects of temperature and flow rate

The effects of feed bulk temperature and feed- and distillate-side flow rates on DCMD performance were investigated. The feedwater contained 0.2 g/L petroleum, 39.3 g/L sodium, 82 g/L chloride, and 12 g/L calcium (TDS at 133 g/L). A new piece of membrane was used in each test. When investigating the effect of feed bulk temperature on DCMD performance, the temperature of the feedwater varied from 40, 60, and 80˚C and the distillate temperature was held at 20˚C. Flow rates of both the feed and distillate streams were maintained at 0.8 L/min. When investigating the effect of flow rate on DCMD performance, flow rates of both streams varied from 0.4 to 2.0 L/min and the feed- and distillate-side bulk temperatures were held at 60 and 20˚C, respectively.

2.3.2. Effect of feedwater composition

The effects of TDS, oil/grease, suspended solids, and volatile organics of the synthetic flowback/produced water on DCMD performance were studied. In each test, the feed temperature was kept at 60˚C and the distillate temperature was held at 20˚C. Flow rates of both streams were maintained at 0.8 L/min. A new piece of membrane was used in each test. The composition of the feedwater used in each study is given in Table 2. For comparison, concentrations of the water compositions reported in literature are also given.

2.4. Membrane foulant identification

The membrane surfaces before and after DCMD testing were analyzed using scanning electron microscopy (SEM; S4800, HITACHI, Japan) to probe the fouling potential. The property of foulants was further identified by comparing the surface functional groups of a virgin membrane, fouled membrane, and petroleum using a Fourier transform infrared (FTIR) spectrometer (Bruker Vector 22, Bruker, UK).

2.5. Effect of methanol

The concentration of methanol inside the distillate was measured using the gas chromatography coupled with a flame ionization detector (GC-FID; 7890A, Agilent Technologies, USA). Methanol rejection was calculated accordingly.

3. Results and discussion

3.1. Effect of feedwater temperature on DCMD performance

Water fluxes of DCMD at different feedwater temperatures for synthetic flowback/produced water treatment are given in Fig. 2. Stable water fluxes were observed over the 5-h test at all the investigated temperatures for both QM038 and GVHP membranes, and more than 99.8% salt rejection was achieved in each test. It can also be seen that the water flux increased from 6 to 43 L/m^2 h for the QM038 membrane and from 3 to 19 L/m^2 h for the GVHP membrane, when

Table 2
Compositions of the synthetic flowback/produced water tested for DCMD

Effect of component to be investigated	Concentration of target component tested in the synthetic water (g/L)	Concentration range of target component found in real flowback/produced water (g/L)			Other components in the synthetic water (g/L)
		Low	Median	High	
TDS	NaCl + $CaCl_2$: 35–335[a]	66 [6] 1 [5]	150 [6] 32 [5]	261 [6] 400 [5]	Petroleum: 0.2
Oil/grease	Petroleum: 0.2 and 1.0	0.01 [6] 0.04 [3] 0.1 [39]	0.018 [6]	0.26 [6] 2.0 [3] 1.0 [39]	TDS: 133[b]
Suspended solids[b]	$CaCO_3$: 0.5 and 2.5 or TiO_2: 0.5 or $BaSO_4$: 0.5[d]	0.001 [5] 0.027 [6]	0.38 [6]	1.0 [5] 3.2 [6]	Petroleum: 0.2 TDS: 133[b]
VOCs	Methanol: 0.025 and 0.05	–	–	0.035 [5] ≤0.039[c] [40]	Petroleum: 0.2 TDS: 133[b]

[a]Varied by adding 0–300 g/L NaCl while keeping Ca concentration constant at 12 g/L; the literature reported an average of 1.5 g/L Ca in real flowback/produced water [5].
[b]Na: 39 g/L, Ca: 12 g/L, and Cl: 82 g/L, making the TDS 133 g/L, representing the medium-level TDS found in real flowback/produced water.
[c]Sum of methanol and ethanol.
[d]The highest concentration of 0.85 g/L was reported in the literature [5].

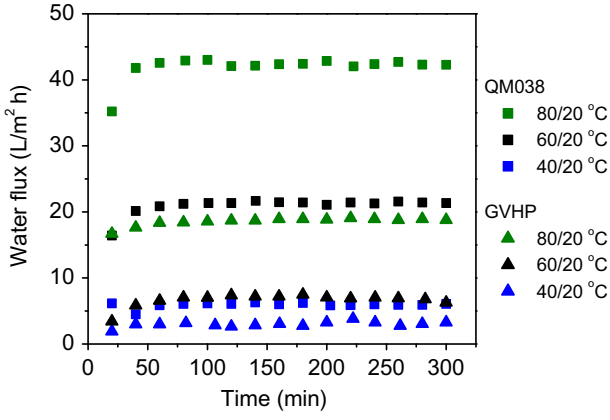

Fig. 2. Water flux of DCMD at different feed temperatures for flowback/produced water treatment (distillate temperature: 20°C; flow rates of both water streams: 0.8 L/min; feedwater composition: 39 g/L sodium, 12 g/L calcium, 82 g/L chloride, and 0.2 g/L oil/grease).

the feedwater temperature increased from 40 to 80°C. The increased water flux at a higher feedwater temperature may be attributed to the greater vapor pressure difference (driving force of DCMD) across the membrane according to the Antoine equation [41]. The reason that the QM038 membrane always showed higher water fluxes than the GVHP membrane is likely because of its much smaller membrane thickness (Table 1) since both membranes have comparable membrane pore size, porosity, and tortuosity (Table 1) and were tested under the same experimental conditions using the same feed solutions. As already known, the experimental condition, feedwater chemistry, and the membrane structure were the factors affecting water flux in DCMD [42]. Therefore, using a highly porous membrane with relatively small pore size and thickness and operated at high feedwater temperatures may be desirable for DCMD to obtain high water flux for the onsite treatment of flowback/produced water.

3.2. *Effect of liquid stream flow rate on DCMD performance*

Water fluxes of DCMD at different feed and distillate stream flow rates are given in Fig. 3. As can be seen, the water flux increases almost linearly with increasing flow rate for both membranes. One possible reason is that more dynamic flow conditions were created inside the membrane module at higher flow

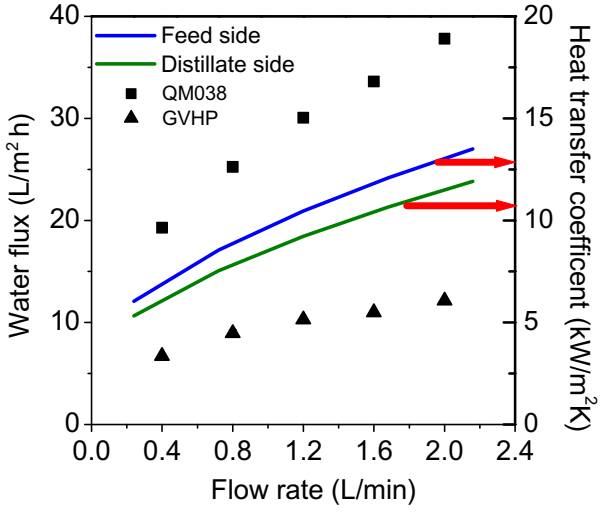

Fig. 3. DCMD performance at different liquid stream flow rates for flowback/produced water treatment (feedwater temperature: 60˚C; distillate temperature: 20˚C; feedwater composition: 39 g/L sodium, 12 g/L calcium, 82 g/L chloride, and 0.2 g/L oil/grease).

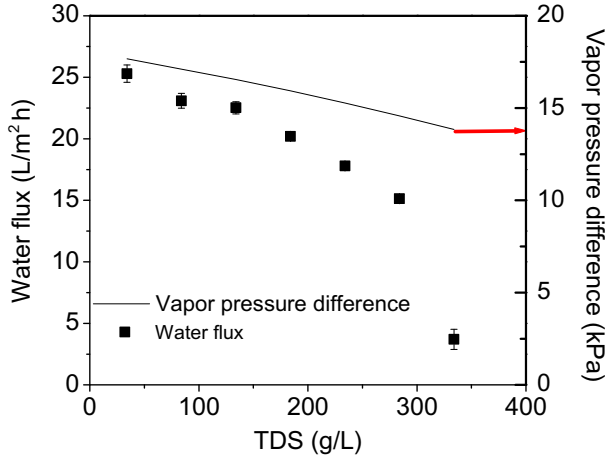

Fig. 4. DCMD performance for the treatment of flowback/produced water with different feed water TDS (feedwater temperature: 60˚C; distillate temperature: 20˚C; flow rates of both water streams: 0.8 L/min; membrane: QM038; feedwater composition: 12 g/L calcium, 0.2 g/L oil/grease, and varied concentrations of sodium and chloride).

rates on both the feed and distillate sides of the membrane, leading to more efficient heat transfer from the bulk solution to the membrane surface; thus, the temperature polarization effect was reduced and water flux was increased [41]. To prove this, heat transfer coefficients on both the feed and distillate sides of the membrane at each liquid stream flow rate were determined (Appendix A) and the results (solid lines in Fig. 3) are consistent with the previous assumption. It should be noted that the flow rates tested in the current bench-scale DCMD system (0.4–2.0 L/min, or 95–476 L/min m^2) are much higher than the flow rates reported in pilot-scale air-gap MD systems (5.4–7.1 L/min m^2 [43,44]). Hence, increasing the flow rate to increase water flux may have limitations in field applications of DCMD. Because the QM038 membrane showed much better performance than the GVHP membrane (Figs. 2 and 3), only the QM038 membrane was used for further testing.

3.3. Effect of feedwater TDS on DCMD performance

Water fluxes of DCMD for the treatment of flowback/produced water with different TDS are shown in Fig. 4. As can be seen, water flux decreased with increasing feedwater TDS, likely due to the reduction of vapor pressure difference (solid line in Fig. 4; calculation given in Appendix B). At a feedwater TDS of 33 g/L, DCMD has a water flux of 25 L/m^2 h, which is relatively lower than the water flux of RO (25–40 L/m^2 h for seawater desalination [43,45]). Although increasing feedwater temperature may improve water flux as demonstrated in Fig. 2, DCMD also suffers from higher specific energy consumption, i.e., tens to thousands of kWh/m^3 for DCMD [46] while 10–20 kWh/m^3 for a small-scale RO [47,48]. Therefore, DCMD may be less competitive than RO for low-TDS flowback/produced water treatment. However, DCMD has an excellent potential for treating medium-to-high TDS flowback/produced water where RO treatment is no longer practical. As shown in Fig. 4, only 14% water flux decline occurred when the feedwater TDS increased from 33 to 150 g/L (median TDS of flowback/produced water reported in [6]). In addition, DCMD is capable of treating flowback/produced water with a TDS as high as 280 g/L and the water fluxes are always greater than 15 L/m^2 h. This corresponds to 46–88% reduction of wastewater volume if the feedwater prior to DCMD treatment has low (33 g/L)-to-medium (150 g/L) TDS levels. Further concentrating the feedwater to 320 g/L, however, led to a sharp flux decline, possibly because the TDS is approaching the NaCl solubility in water. A similar phenomenon was also observed in another literature report treating the Great Salt Lake water with DCMD; when the feedwater TDS exceeded 300 g/L, the homogeneous precipitation of NaCl caused a rapid flux decline [49]. The tested membrane was analyzed under SEM-EDS, and large quantities of crystals with typical NaCl structure were observed on

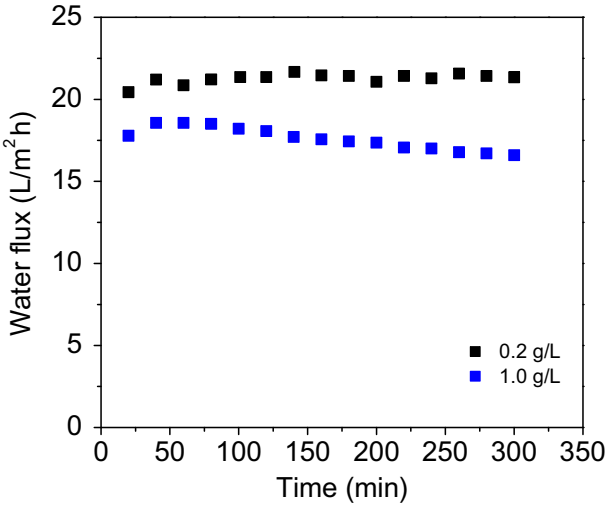

Fig. 5. Water flux of DCMD for the treatment of flowback/produced water with different oil/grease concentrations (feed temperature: 60°C; distillate temperature: 20°C; flow rates of both water streams: 0.8 L/min; membrane: QM038; feedwater composition: 39 g/L sodium, 12 g/L calcium, 82 g/L chloride, and 0.2 or 1.0 g/L oil/grease).

the membrane surface (Appendix C). EDS further confirmed the crystal elements as mainly Na and Cl (Appendix C). The distillate conductivity was recorded during each test and less than 20 μS/cm was measured in the current study.

3.4. Effect of oil/grease on DCMD performance

In these tests, the feedwater contains oil/grease, 39 g/L sodium, 12 g/L calcium, and 82 g/L chloride (Table 2) to represent the medium-level TDS found in real flowback/produced water. For feedwater containing 0.2 and 1.0 g/L oil/grease, the particle size of the oil-in-water emulsions was in the range of 140–300 nm (average of 220 nm) and 255–400 nm (average of 295 nm), respectively. Oil emulsions with these small sizes in the flowback/produced water are difficult to be removed by traditional methods [37]. However, the water flux results in Fig. 5 suggest that DCMD is very effective to treat wastewater containing small oil emulsions: no flux decline at an oil/grease concentration of 0.2 g/L and only 11% flux

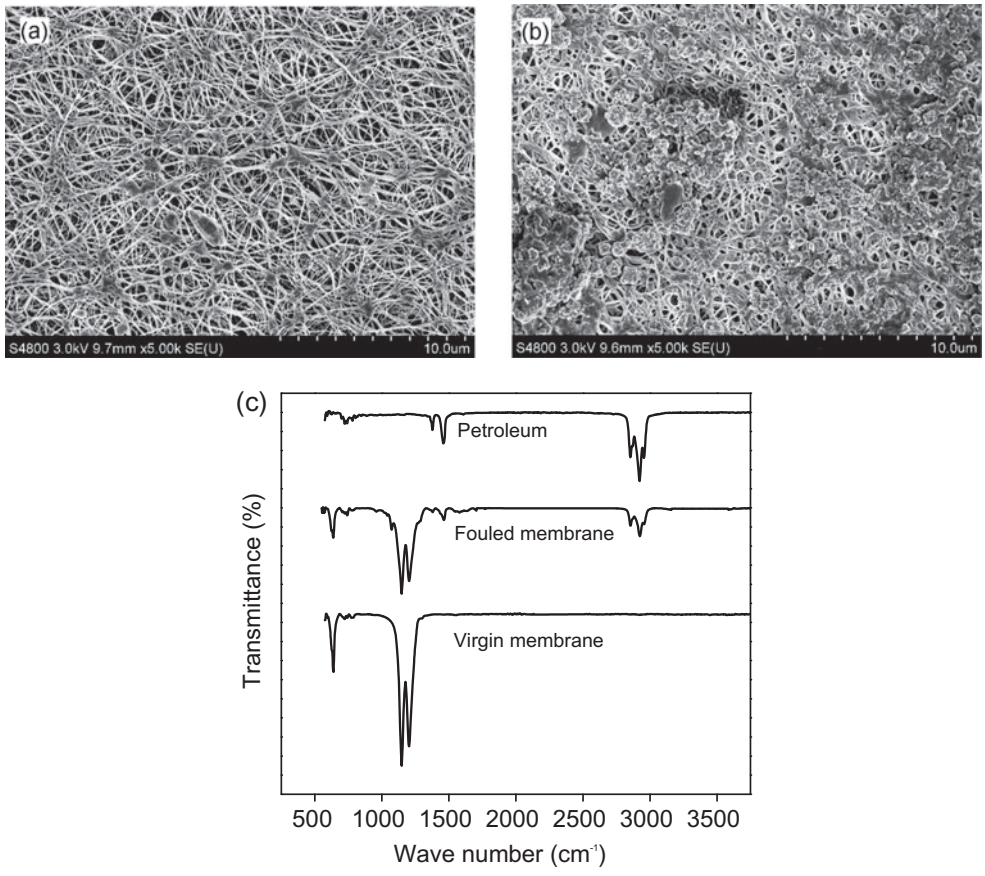

Fig. 6. Identification of the presence of foulants on membrane surface: SEM image of a virgin membrane surface (a), SEM image of the fouled membrane surface (b), and FTIR of membranes and petroleum (c).

decline at an oil/grease concentration of 1.0 g/L (highest concentration reported in real flowback/produced water [39]) at the end of the 5-h test. The flux decline is likely due to membrane fouling caused by the attachment of insoluble aromatics (component of oil/grease) onto the membrane surface especially at the edge areas (Appendix D). To verify the presence of membrane foulant on these areas, membrane surfaces of a virgin membrane and the fouled membrane areas were analyzed under SEM and different membrane polymeric structures were observed (Fig. 6). The foulant was further confirmed to be from petroleum by comparing the functional groups of the foulant, the virgin membrane, and the petroleum using FTIR (Fig. 6(c)), where typical functional groups of petroleum at wave numbers of 1,500 and 3,000 cm^{-1} were observed on the fouled membrane surface but not on the virgin membrane. The slight decline in water flux in Fig. 5 suggests that only part of the membrane surface was fouled with the 1.0 g/L oil/grease feedwater.

The distillate conductivity was less than 20 μS/cm at the end of the 5-h test for the 0.2 g/L oil/grease feedwater treatment but almost 200 μS/cm for the 1.0 g/L oil/grease feedwater treatment. The components of the high-conductivity distillate were further analyzed to be 117.9 mg/L petroleum using a TOC analyzer (TOC-5000A, Shimadzu, Japan), 47.6 mg/L chloride using an ion chromatography system (ICS-1000, Dionex), 23.7 mg/L sodium and 7.54 mg/L calcium using Atomic Absorption Spectroscopy (iCE 3000, Thermo Scientific). The relatively high distillate conductivity, 200 μS/cm, suggests membrane wetting had occurred in the testing of 1.0 g/L oil/grease feedwater. The high petroleum concentration of the distillate may be attributed to both membrane wetting caused by the chemical additives such as natural surfactants inside the oil and grease [50] and the volatile property of petroleum. It should be noted that an oil/grease concentration as high as 1.0 g/L was used here, which is at the maximum limit observed in some real flowback/produced water (Table 2); therefore, less severe membrane wetting phenomenon (thus low petroleum and salt concentrations in distillate) is expected for real flowback/produced water treatment using DCMD.

3.5. Effect of suspended solids on DCMD performance

Membrane scaling caused by deposition of $CaCO_3$ on membrane surface has been frequently reported in DCMD [33,51]; suspended $CaCO_3$ was also observed in flowback/produced water [6]. Therefore, the effect of $CaCO_3$ on DCMD performance was investigated here. Results are given in Fig. 7. As can be seen, the water flux decreased gradually within the first 3 h (10–17% flux decline for both tests; black and blue solid squares in Fig. 7), likely due to membrane pore blocking by the $CaCO_3$ particles. A stable water flux was observed in the next 6 h in each test, suggesting that the pore blocking effect might have reached the maximum after 3 h. Therefore, the suspended $CaCO_3$ particles have a minimal effect on DCMD performance. The overall particle size distribution of $CaCO_3$ was not measured because of quick sedimentation of large $CaCO_3$ particles. After removing the $CaCO_3$ sediments, the suspended particles were found to have sizes in the range of 1–2 μm. The membrane after testing was analyzed by SEM–EDS (Appendix E). Particles in the size of 1–3 μm were observed on the membrane surface, in agreement with the particle size measurement by the Zetasizer. The EDS result suggested the particles were likely $CaCO_3$ and NaCl. A feedwater containing 2.5 g/L $CaCO_3$ particles was further tested at a higher flow rate (1.5 L/min; hollow squares in Fig. 7) and similar to that at lower flow rate (0.8 L/min), almost 10% flux decline occurred within the first 2 h and after that, the flux kept almost constant. This result suggests that increasing the shear stress by elevating the water stream flow rate (to 1.5 L/min in the current study) is not sufficient to remove the particles attached on the membrane surface.

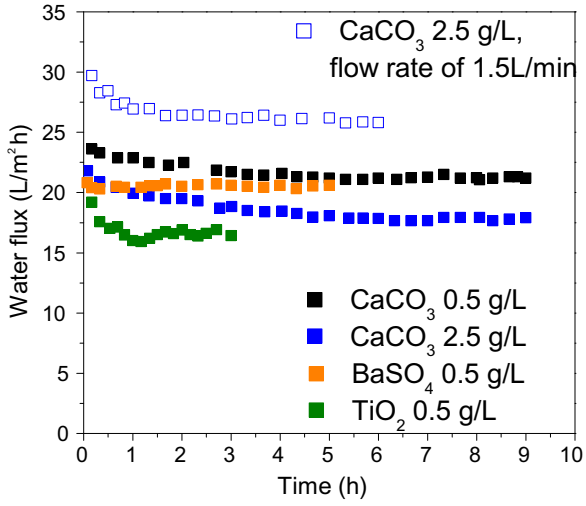

Fig. 7. DCMD performance for treatment of flowback/produced water with suspended $CaCO_3$, $BaSO_4$, and TiO_2 particles (feed temperature: 60°C; distillate temperature: 20°C; flow rates of both streams: 0.8 L/min for solid symbol tests and 1.5 L/min for hollow symbol test; membrane: QM038; feedwater composition: 39 g/L sodium, 12 g/L calcium, 82 g/L chloride, 0.2 g/L oil/grease, and varied concentrations of suspended particles).

Table 3
DCMD performance for treatment of flowback/produced water containing methanol (feedwater temperature: 60°C; distillate temperature: 20°C; flow rates of both water streams: 0.8 L/min; membrane: QM038; feedwater composition: 39 g/L sodium, 12 g/L calcium, 82 g/L chloride, 0.2 g/L oil/grease, and varied methanol concentrations)

Initial methanol concentration (ppm)	Water flux (L/m^2 h)	Methanol rejection (%)	Salt rejection (%)
0	21.2 ± 0.4	–	99.95
25	21.3 ± 0.7	52.8 ± 2.9	99.99
50	21.4 ± 0.7	63.2 ± 3.5	99.98

Besides $CaCO_3$, precipitation of barium sulfate and strontium sulfate was also observed during the flowback/produced water treatment process [6]; therefore, the effect of barium sulfate ($BaSO_4$) on DCMD performance was also investigated in this work. Unlike $CaCO_3$ where slight flux decline occurred at the beginning of the test, almost no flux decline was observed during the entire test (orange squares in Fig. 7). Therefore, the suspended $BaSO_4$ particles in the flowback/produced water also have a minimal effect on DCMD. The particle size distribution of $BaSO_4$ was measured as 250–650 nm with an average of 460 nm.

To investigate the effect of particle size of suspended solids on DCMD performance, another feed solution containing 0.5 g/L TiO_2 nanoparticles was also studied (composition in Table 2). This solution has particle sizes of 1,100–1,700 nm with an average size of 1,281 nm, which are smaller than the particle sizes of the $CaCO_3$ solution but much greater than the sizes of the $BaSO_4$ particles and TiO_2 nanoparticles (~25 nm according to the manufacturer); therefore, aggregation of TiO_2 nanoparticles has occurred inside the feed solution. Water flux results of the feed solution containing suspended TiO_2 are given in Fig. 7 (green squares). As can be seen, 17% flux decline occurred within the first hour; after that, the flux kept almost constant. Similar to the flux phenomenon of the $CaCO_3$ solution, membrane scaling caused by the TiO_2 particles also occurred only at the beginning of the test and no more membrane scaling occurred with a longer test time. The current study suggests that suspended solids inside the flowback/produced water have a minimal effect on DCMD performance. This result together with Fig. 5 indicates that pretreatment processes for removal of suspended solids and oil/grease may not be necessary in DCMD.

3.6. Effect of volatile organics on DCMD performance

Volatile organics in the flowback/produced water may enter into drinking water sources (e.g. groundwater, surface water) or emit into air and cause adverse health effect on human beings [40]. In this study, methanol was used as a representative of volatile organics because it is frequently dosed in fracking fluids as a scale inhibitor, nonemulsifier, and corrosion inhibitor [40], yet its effect on DCMD performance is still unknown. Test results are given in Table 3. As can be seen, the salt rejections are all greater than 99.95%, suggesting no membrane wetting caused by methanol occurred. In addition, stable water fluxes were observed during the 2-h test (results not shown), indicating no membrane fouling occurred, which is likely because of the very low concentration of methanol. However, poor methanol rejections (53 and 63%) were observed, likely due to its volatile property. The current test results conducted at representing of VOC levels (0.39–50 mg/L present in real flowback/produced water [5]) suggest the presence of VOCs such as methanol in fracking fluids may not affect the performance of DCMD, although the distillate may still contain VOCs.

4. Conclusion

This bench-scale study found DCMD technically feasible to treat synthetic flowback/produced water from the oil and gas field. Both feedwater temperature and liquid stream flow rates significantly affected water flux. Oil/grease, suspended solids, and volatile organics showed minimal effects on DCMD membrane fouling and scaling; therefore, no pretreatment process is necessary for flowback/produced water treatment in DCMD. This study also suggests that DCMD has a water flux comparable to RO when treating low-TDS flowback/produced water, but the high energy consumption of DCMD makes it less attractive than RO to be applied in the field. When treating medium-to-high TDS flowback/produced water that cannot be processed by RO, DCMD is technically feasible. The high-quality distillate may be reused for industrial and agricultural applications. Therefore, DCMD may have potential to be applied onsite for real medium-to-high TDS flowback/produced water treatment in the oil and gas field.

Acknowledgment

This work is supported by the Water Catalyst Grant Program at the University of Wisconsin-Milwaukee and by the new faculty startup fund at Texas A&M University.

References

[1] B.D. Coday, P. Xu, E.G. Beaudry, J. Herron, K. Lampi, N.T. Hancock, T.Y. Cath, The sweet spot of forward osmosis: Treatment of produced water, drilling wastewater, and other complex and difficult liquid streams, Desalination 333 (2014) 23–35.
[2] B.G. Rahm, S.J. Riha, Toward strategic management of shale gas development: Regional, collective impacts on water resources, Environ. Sci. Policy 17 (2012) 12–23.
[3] C.E. Clark, J.A. Veil, Produced water volumes and management practices in the United States, in, Environmental Science Division, Argonne National Laboratory, Lemont, IL, 2009.
[4] F. Ahmadun, A. Pendashteh, L.C. Abdullah, D.R.A. Biak, S.S. Madaeni, Z.Z. Abidin, Review of technologies for oil and gas produced water treatment, J. Hazard. Mater. 170 (2009) 530–551.
[5] K.L. Benko, J.E. Drewes, Produced water in the Western United States: Geographical distribution, occurrence, and composition, Environ. Eng. Sci. 25(2) (2008) 239–246.
[6] K.B. Gregory, R.D. Vidic, D.A. Dzombak, Water management options associated with the production of shale gas by hydraulic fracturing, Elements 7 (2012) 181–186.
[7] G.L. Theodori, A.E. Luloff, F.K. Willits, D.B. Burnett, Hydraulic fracturing and the management, disposal, and reuse of frac flowback waters: Views from the public in the Marcellus Shale ERSS 2 (2014) 66–74.
[8] S.S. Hutson, N.L. Barber, J.F. Kenny, K.S. Linsey, D.S. Lumia, M.A. Maupin, Estimated use of water in the United States in 2000, USGS Circular 1268 (2004) 44–46.
[9] S. Mondal, S.R. Wickramasinghe, Produced water treatment by nanofiltration and reverse osmosis membranes, J. Membr. Sci. 322 (2008) 162–170.
[10] J. Chen, M.H. Al-Wadei, R.C.M. Kennedy, P.D. Terry, Hydraulic fracturing: Paving the way for a sustainable future? J. Environ. Public Health 2014 (2014) 1–10.
[11] S. Rassenfoss, From flowback to fracturing: Water recycling grows in the marcellus shale, J. Petrol. Technol. 63 (2011) 48–51.
[12] J.A. Veil, M.G. Puder, D. Elcock, R.J. Redweik, A White Paper Describing Produced Water from Preoduction of Crude Oil, Natural Gas, and Coal Bed Methane, Argonne National Laboratory, Lemont, IL, 2004.
[13] Q. Jiang, J. Rentschler, R. Perrone, K. Liu, Application of ceramic membrane and ion-exchange for the treatment of the flowback water from Marcellus shale gas production, J. Membr. Sci. 431 (2013) 55–61.
[14] G. Chen, Z. Wang, L.D. Nghiem, X. Li, M. Xie, B. Zhao, M. Zhang, J. Song, T. He, Treatment of shale gas drilling flowback fluids (SGDFs) by forward osmosis: Membrane fouling and mitigation, Desalination 366 (2015) 113–120.
[15] R.M. Abousnina, L.D. Nghiem, J. Bundschuh, Comparison between oily and coal seam gas produced water with respect to quantity, characteristics and treatment technologies: A review, Desalin. Water Treat. 54 (2015) 1793–1808.
[16] B.D. Coday, N. Almaraz, T.Y. Cath, Forward osmosis desalination of oil and gas wastewater: Impacts of membrane selection and operating conditions on process performance, J. Membr. Sci. 488 (2015) 40–55.
[17] X.M. Li, B. Zhao, Z. Wang, M. Xie, J. Song, L.D. Nghiem, T. He, C. Yang, C. Li, G. Chen, Water reclamation from shale gas drilling flow-back fluid using a novel forward osmosis-vacuum membrane distillation hybrid system, Water Sci. Technol. 69(5) (2014) 1036–1044.
[18] D.L. Shaffer, L.H.A. Chavez, M. Ben-Sasson, S.R. Castrillón, N.Y. Yip, M. Elimelech, Desalination and reuse of high-salinity shale gas produced water: Drivers, technologies, and future directions, Environ. Sci. Technol. 47(17) (2013) 9569–9583.
[19] A.G. Fane, R.W. Schofield, C.J.D. Fell, The efficient use of energy in membrane distillation, Desalination 64 (1987) 231–243.
[20] S. Alobaidani, E. Curcio, F. Macedonio, G. Diprofio, H. Alhinai, E. Drioli, Potential of membrane distillation in seawater desalination: Thermal efficiency, sensitivity study and cost estimation, J. Membr. Sci. 323 (2008) 85–98.
[21] H. Susanto, Towards practical implementations of membrane distillation, Chem. Eng. Process. 50 (2011) 139–150.
[22] M. Gryta, Concentration of saline wastewater from the production of heparin, Desalination 129 (2000) 35–44.
[23] A. El-Abbassi, A. Hafidi, M.C. García-Payo, M. Khayet, Concentration of olive mill wastewater by membrane distillation for polyphenols recovery, Desalination 245 (2009) 670–674.
[24] P.P. Zolotarev, V.V. Ugrozov, I.B. Volkina, V.M. Nikulin, Treatment of waste water for removing heavy metals by membrane distillation, J. Hazard. Mater. 37 (1994) 77–82.
[25] C.R. Martinetti, A.E. Childress, T.Y. Cath, High recovery of concentrated RO brines using forward osmosis and membrane distillation, J. Membr. Sci. 331 (2009) 31–39.
[26] F. Edwie, T.S. Chung, Development of hollow fiber membranes for water and salt recovery from highly concentrated brine via direct contact membrane distillation and crystallization, J. Membr. Sci. 421–422 (2012) 111–123.
[27] K.W. Lawson, D.R. Lloyd, Membrane distillation. II. Direct contact MD, J. Membr. Sci. 120 (1996) 123–133.
[28] H.C. Duong, A.R. Chivas, B. Nelemans, M. Duke, S. Gray, T.Y. Cath, L.D. Nghiem, Treatment of RO brine from CSG produced water by spiral-wound air gap membrane distillation—A pilot study, Desalination 366 (2015) 121–129.
[29] A. Alkhudhiri, N. Darwish, N. Hilal, Produced water treatment: Application of air gap membrane distillation, Desalination 309 (2013) 46–51.
[30] S. Nakao, Determination of pore size and pore size distribution, J. Membr. Sci. 96 (1994) 131–165.
[31] S. Adnan, M. Hoang, H. Wang, Z. Xie, Commercial PTFE membranes for membrane distillation application: Effect of microstructure and support material, Desalination 284 (2012) 297–308.

[32] L.D. Nghiem, T. Cath, A scaling mitigation approach during direct contact membrane distillation, Sep. Purif. Technol. 80 (2011) 315–322.
[33] M. Gryta, Fouling in direct contact membrane distillation process, J. Membr. Sci. 325 (2008) 383–394.
[34] M. Gryta, Desalination of thermally softened water by membrane distillation process, Desalination 257 (2010) 30–35.
[35] D. Singh, K.K. Sirkar, Desalination of brine and produced water by direct contact membrane distillation at high temperatures and pressures, J. Membr. Sci. 389 (2012) 380–388.
[36] F. Macedonio, A. Ali, T. Poerio, E. El-Sayed, E. Drioli, Direct contact membrane distillation for treatment of oilfield produced water, Sep. Purif. Technol. 126 (2014) 69–81.
[37] S. Zhang, P. Wang, X. Fu, T. Chung, Sustainable water recovery from oily wastewater via forward osmosis-membrane distillation (FO-MD), Water Res. 52 (2014) 112–121.
[38] G. Rao, S.R. Hiibel, A.E. Childress, Simplified flux prediction in direct-contact membrane distillation using a membrane structural parameter, Desalination 351 (2014) 151–162.
[39] B. Chakrabarty, A.K. Ghoshal, M.K. Purkait, Cross-flow ultrafiltration of stable oil-in-water emulsion using polysulfone membranes, Chem. Eng. J. 165 (2010) 447–456.
[40] T. Saba, F. Mohsen, M.G arry, B. Murphy, B. Hilbert, White Paper Methanol Use in Hydraulic Fracturing Fluids, Exponent, Maryland, MA, 2012.
[41] R.W. Schofield, A.G. Fane, C.J.D. Fell, Heat and mass transfer in membrane distillation, J. Membr. Sci. 33 (1987) 299–313.
[42] A.O. Imdakm, T. Matsuura, Simulation of heat and mass transfer in direct contact membrane distillation (MD): The effect of membrane physical properties, J. Membr. Sci. 262 (2005) 117–128.
[43] E. Guillén-Burrieza, J. Blanco, G. Zaragoza, D. Alarcón, P. Palenzuela, M. Ibarra, W. Gernjak, Experimental analysis of an air gap membrane distillation solar desalination pilot system, J. Membr. Sci. 379 (2011) 386–396.
[44] J. Minier-Matar, A. Hussain, A. Janson, F. Benyahia, S. Adham, Field evaluation of membrane distillation technologies for desalination of highly saline brines, Desalination 351 (2014) 101–108.
[45] K.P. Lee, T.C. Arnot, D. Mattia, A review of reverse osmosis membrane materials for desalination—Development to date and future potential, J. Membr. Sci. 370 (2011) 1–22.
[46] M. Khayet, Solar desalination by membrane distillation: Dispersion in energy consumption analysis and water production costs (a review), Desalination 308 (2013) 89–101.
[47] M. Thomson, M.S. Miranda, D. Infield, A small-scale seawater reverse-osmosis system with excellent energy efficiency over a wide operating range, Desalination 153 (2002) 229–236.
[48] B. Peñate, L. García-Rodríguez, Current trends and future prospects in the design of seawater reverse osmosis desalination technology, Desalination 284 (2012) 1–8.
[49] K.L. Hickenbottom, T.Y. Cath, Sustainable operation of membrane distillation for enhancement of mineral recovery from hypersaline solutions, J. Membr. Sci. 454 (2014) 426–435.
[50] B. Chakrabarty, A.K. Ghoshal, M.K. Purkait, Ultrafiltration of stable oil-in-water emulsion by polysulfone membrane, J. Membr. Sci. 325 (2008) 427–437.
[51] D. Qu, J. Wang, B. Fan, Z. Luan, D. Hou, Study on concentrating primary reverse osmosis retentate by direct contact membrane distillation, Desalination 247 (2009) 540–550.
[52] N.B. Vargaftik, L.P. Filippov, A.A. Tarzimanov, E.E. Totskii, Handbook of Thermal Conductivity of Liquids and Gases, CRC Press, Boca Raton, FL, 1993.
[53] G. Rao, S.R. Hiibel, A. Achilli, A.E. Childress, Factors contributing to flux improvement in vacuum-enhanced direct contact membrane distillation, Desalination 367 (2015) 197–205.

Appendix A

Heat transfer coefficients (h) were determined by:

$$h = \frac{\mathrm{Nu}\ k_\mathrm{f}}{d_\mathrm{h}} \tag{A1}$$

where k_f is the thermal conductivity of the fluid (0.646 W/m K for feed and 0.604 W/m K for distillate [52]) and d_h is the hydraulic diameter of the flow channel on the feed or distillate side (2.508 mm). Nu is the Nusselt number, which for a spacer-filled channel was determined by [53]:

$$\mathrm{Nu} = 0.664 k_\mathrm{dc}\,\mathrm{Re}^{0.5}\,\mathrm{Pr}^{0.33}\left(\frac{2d_\mathrm{h}}{l_\mathrm{m}}\right)^{0.5} \tag{A2}$$

where Re is the Reynolds number (690.4 at feed and 367.8 at distillate); Pr is the Prandtl number (4.49 at feed and 7.58 at distillate); and l_m is the mesh size of the spacer (7 mm). k_dc was determined by [53]:

$$k_\mathrm{dc} = 1.654\left(\frac{d_\mathrm{f}}{H}\right)^{-0.039}\varepsilon_\mathrm{s}^{0.75}\left(\sin\frac{\theta_\mathrm{s}}{2}\right)^{0.086} \tag{A3}$$

where d_f is the spacer filament size (0.5 mm); H is the channel height (0.105 cm); ε_s is the spacer porosity (96%); and θ_s is the hydrodynamic angle of the spacer, which is the angle formed by the grids of the spacer (60°).

Appendix B

Vapor pressure difference (ΔP) at each TDS of the feed solution was calculated by [53]:

$$\Delta P = P_\mathrm{f} - P_\mathrm{d} \tag{B1}$$

where P_f and P_d are the vapor pressures at the feed and distillate sides, respectively. P_f and P_d were determined by:

$$P_f = \exp\left(23.328 - \frac{3841}{T_f - 45}\right)(1 - x)(1 - 0.5x - 10x^2) \quad \text{(B2)}$$

$$P_d = \exp\left(23.328 - \frac{3841}{T_d - 45}\right) \quad \text{(B3)}$$

where T_f and T_d are the feed (60°C) and distillate-side (20°C) temperatures and x is the molar fraction of the dissolved salts inside the feed solution (function of TDS: 0.03077 × TDS).

Appendix C

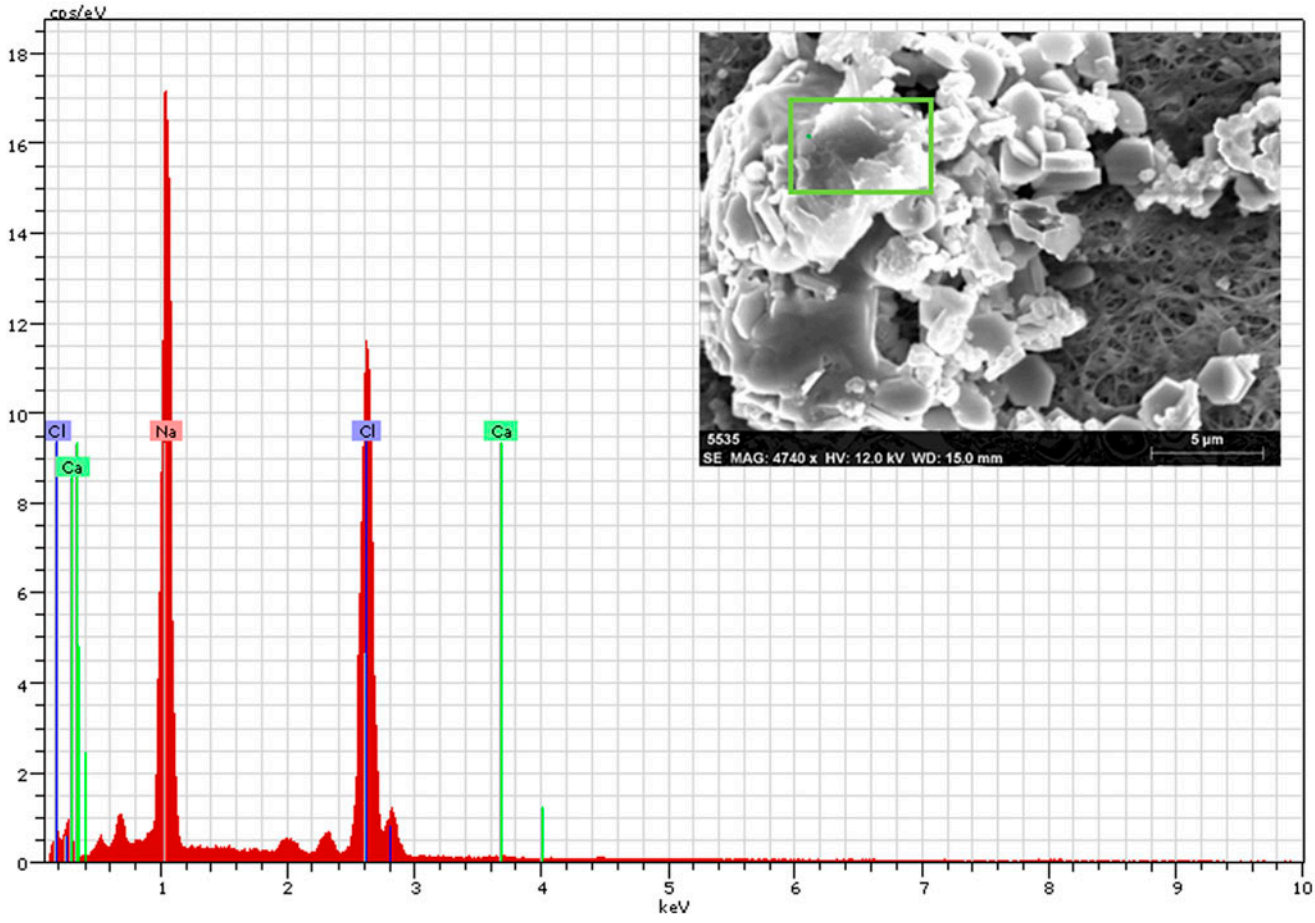

SEM–EDS analysis of the membrane surface after tested at a feedwater TDS of 320 g/L: typical crystals observed on membrane surface (a) and elementary analysis of the crystals (b).

Appendix D

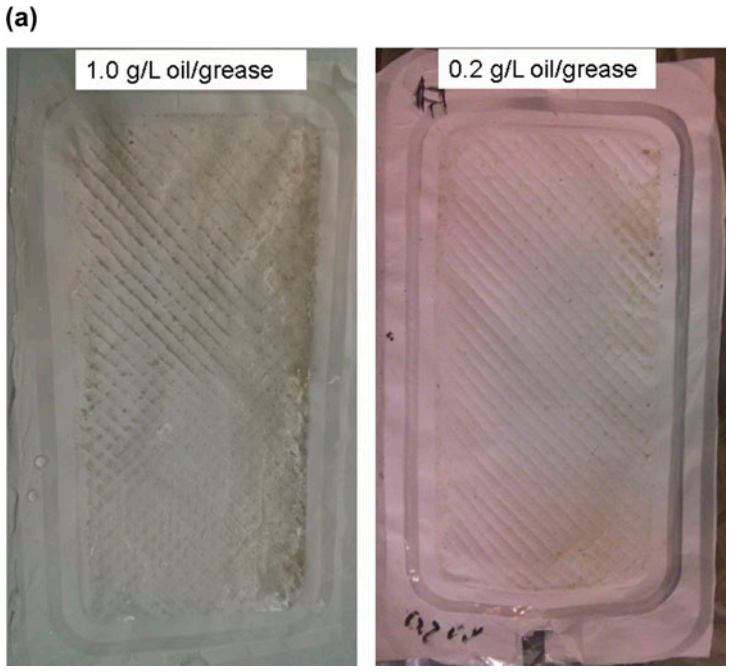

Photographs of membranes after the DCMD test in Section 3.4.

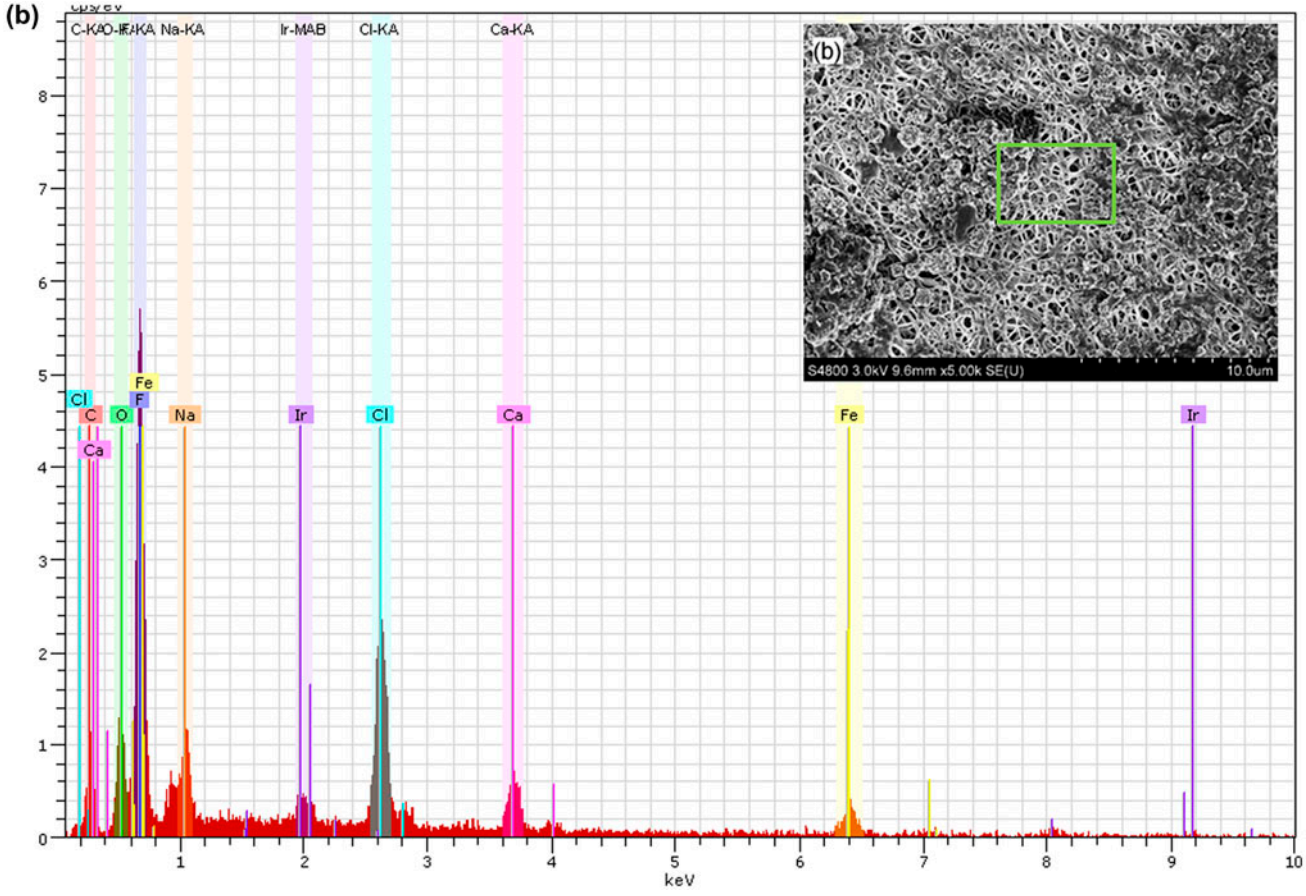

SEM–EDS analysis of the membrane tested in feedwater containing 1.0 g/L oil/grease.

Appendix E

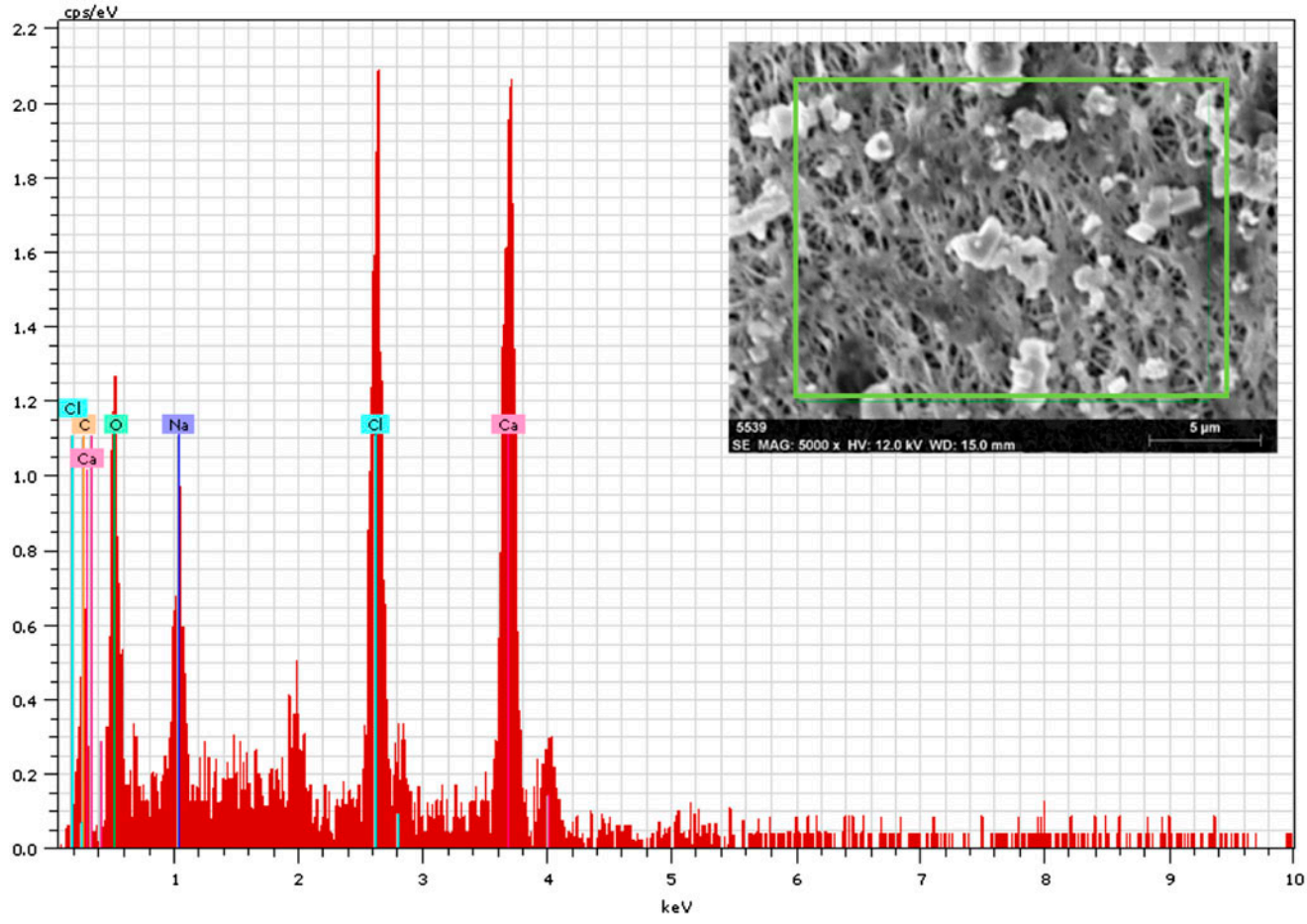

SEM–EDS analysis of the membrane tested in feedwater containing suspended $CaCO_3$.